AIP Applied Physics Letters

Tunable exchange bias-like effect in patterned hard-soft two-dimensional lateral composites with perpendicular magnetic anisotropy

A. Hierro-Rodriguez, J. M. Teixeira, M. Vélez, L. M. Alvarez-Prado, J. I. Martín, and J. M. Alameda

Citation: Applied Physics Letters **105**, 102412 (2014); doi: 10.1063/1.4895771
View online: http://dx.doi.org/10.1063/1.4895771
View Table of Contents: http://scitation.aip.org/content/aip/journal/apl/105/10?ver=pdfcov
Published by the AIP Publishing

APPLIED PHYSICS LETTERS **105**, 102412 (2014)

Tunable exchange bias-like effect in patterned hard-soft two-dimensional lateral composites with perpendicular magnetic anisotropy

A. Hierro-Rodriguez,[1,2,a)] J. M. Teixeira,[3] M. Vélez,[1] L. M. Alvarez-Prado,[1,2] J. I. Martín,[1,2] and J. M. Alameda[1,2]

[1]*Departamento de Física, Universidad de Oviedo, C/Calvo Sotelo S/N, 33007 Oviedo, Spain*
[2]*Centro de Investigación en Nanomateriales y Nanotecnología—CINN (CSIC—Universidad de Oviedo—Principado de Asturias), Parque Tecnológico de Asturias, 33428 Llanera, Spain*
[3]*IN-IFIMUP, Departamento de Física e Astronomia, Faculdade de Ciências, Universidade do Porto, Rua Campo Alegre 687, 4169-007 Porto, Portugal*

(Received 21 March 2014; accepted 3 September 2014; published online 12 September 2014)

Patterned hard-soft 2D magnetic lateral composites have been fabricated by e-beam lithography plus dry etching techniques on sputter-deposited $NdCo_5$ thin films with perpendicular magnetic anisotropy. Their magnetic behavior is strongly thickness dependent due to the interplay between out-of-plane anisotropy and magnetostatic energy. Thus, the spatial modulation of thicknesses leads to an exchange coupled system with hard/soft magnetic regions in which rotatable anisotropy of the thicker elements provides an extra tool to design the global magnetic behavior of the patterned lateral composite. Kerr microscopy studies (domain imaging and magneto-optical Kerr effect magnetometry) reveal that the resulting hysteresis loops exhibit a tunable exchange bias-like shift that can be switched on/off by the applied magnetic field. © *2014 AIP Publishing LLC*.
[http://dx.doi.org/10.1063/1.4895771]

Patterned magnetic media have been the focus of an intense research during the last decade due not only to fundamental physical interest but also because of their potential for technological applications.[1–7] Usually, these systems consist in arrays of structures, where the magnetic behavior is studied as a function of shape and/or structures density without changing the intrinsic magnetic properties. The use of magnetic lateral multilayers, i.e., extended films with a 1D lateral modulation of intrinsic magnetic properties, such as magnetic anisotropy,[8] saturation magnetization,[9] or exchange bias,[10] introduces an extra freedom degree, which should be useful in the development of forefront magnetic devices. The combination of different exchange coupled materials gives rise to many interesting phenomena in standard vertical multilayers such as standard exchange bias in antiferromagnetic/ferromagnetic systems[11,12] or isothermal field induced exchange bias effects in coupled ferromagnetic bilayers with orthogonal anisotropies.[13–16] A lateral exchange coupled configuration could be used to reproduce these phenomena. For example, exchange-spring behavior has been demonstrated in soft-magnetic films with laterally modulated saturation magnetization[9] and misfit strain has been shown to take a central role in the magnetic configuration of stripe domains in weak perpendicular magnetic anisotropy lateral multilayers.[17] This lateral approach can be taken a step further with the design of 2D lateral structures on continuous magnetic films: ordered 2D arrays of hard magnetic elements (Co and CoPt) coupled to soft permalloy films have been used to modify its magnetization reversal process through magnetostatic interactions;[18,19] also, out-of-plane exchange bias effects have been demonstrated in arrays of CoPt platelets coupled to a continuous CoPt film with strong perpendicular magnetic anisotropy.[20]

In this framework, magnetic materials with weak perpendicular magnetic anisotropy (PMA),[21] such as thin films of amorphous NdCo alloys, present several interesting features for the design of 2D hard/soft lateral composites since their magnetic behavior is strongly thickness dependent due to the interplay between out-of-plane anisotropy and magnetostatic energy.[22] Below a critical thickness, they show a soft magnetic behavior with in-plane magnetization; however, above this critical thickness, weak stripe domains are nucleated in the magnetic film, which implies a significant hardening of in-plane hysteresis loops and the onset of the so-called rotatable anisotropy.[23] Thus, lateral thickness variations provide a simple way to create a pattern of exchange coupled hard/soft regions within the sample.[17] Even more, the in-plane easy axis of rotatable anisotropy is determined by the direction of the last saturating magnetic field.[24] Thus, in-plane magnetic anisotropy in the hard regions can be tuned through magnetic history, which adds to the flexibility of the design of the final hard/soft composite.

In this work, we report the fabrication of soft 2D $NdCo_5$-based magnetic lateral hard/soft composites as sketched in Fig. 1(a). The samples consist in patterned microstructure arrays of $NdCo_5$ discs with 3 μm diameter and 60 nm of thickness, arranged in a square lattice geometry and exchange-coupled to a $NdCo_5$ etched film with 30 nm of thickness. This highly symmetric 2D design allows us to take advantage of rotatable anisotropy to control the magnetic response of these systems by the orientation of the last saturating magnetic field. Actually, we observe an "exchange bias-like" shift (H_b) of few Oe in the in-plane magnetization hysteresis cycles [$M(H)$] of the $NdCo_5$ etched film tunable through magnetic history.

[a)]Electronic mail: ahierro@fc.up.pt Present address: IN-IFIMUP and INESC TEC (coordinated by INESC Porto), Departamento de Física e Astronomia, Faculdade de Ciências, Universidade do Porto, Rua Campo Alegre 687, 4169-007 Porto, Portugal.

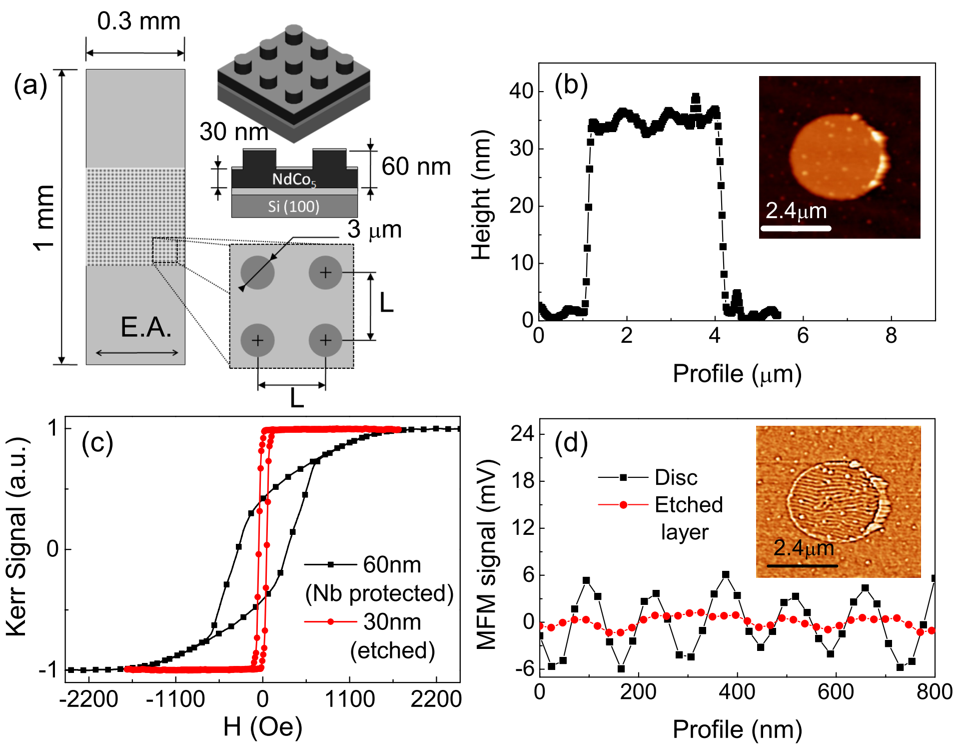

FIG. 1. (a) Scheme of the $NdCo_5$ discs patterned arrays. (b) Atomic force microscopy (AFM) profile of a disc and surrounding layer (image at inset). (c) In-plane hysteresis loops measured by transverse magneto-optical Kerr effect of the continuous $NdCo_5$ control samples showing the Nb protected and etched layers. (d) Magnetic force microscopy (MFM) profiles of both, disc and surrounding etched layer (image at inset).

The samples have been fabricated by the combination of electron beam lithography (EBL), sputtering deposition, and ion milling techniques similar to the process described in Ref. 25. The patterned microstructures consist of rectangular $300 \times 1000\,\mu m^2$ magnetic frames, where the central square area of $300 \times 300\,\mu m^2$ is filled with 3 μm diameter discs, in a square lattice with different lattice parameters L (6, 7.5, and 9 μm) and different thicknesses regarding to the rest of the layer [Fig. 1(a)]. First of all, a first EBL process defines a positive resist mask of Poly(methyl methacrylate) (PMMA) 950 K A4 from Microchem^{TM} with thickness of ~200 nm. After sputtering deposition and lift-off processes, the desired magnetic frames with the following layer structure: Si(100)/Al (10 nm)/$NdCo_5$ (60 nm)/Al (3 nm) are obtained. Then, a second EBL process is performed to create an array of 12 nm thick Nb discs, again by sputtering deposition and lift-off, over the center of the magnetic frame, which will act as a protective mask during an Ar^+ ion milling. In this way, we get, after the milling of the complete Nb layer, an exchange coupled system of 60 nm thick $NdCo_5$ discs within 30 nm thick $NdCo_5$ etched layer [Fig. 1(b)]. Finally, a 3 nm Al protective layer is sputter deposited over the whole sample to prevent oxidation. During this process, continuous control samples have been fabricated within the microstructures following all fabrication steps mentioned above. These unpatterned samples consist, after an Ar^+ ion milling process, in full films of $NdCo_5$ with 60 and 30 nm of thickness. In the former case, the sample was coated with 12 nm Nb protective layer.

Figure 1(c) shows the resulting hysteresis loops in the control continuous layers sputter deposited at the same time that the 2D micro-composite, measured by transverse magneto-optical Kerr effect (T-MOKE),[26] where the applied magnetic field direction is parallel to the in-plane E.A. Depending on the thickness of the magnetic layer, the magnetic hysteresis loop of the system can change from a clear transcritical loop (a reduced in-plane remanent magnetization followed by an almost linear reversible region as the magnetization approaches to saturation) with remarkable PMA (Nb protected layer), to an in-plane uniaxial loop (etched layer) with a reduction in coercivity from 300 Oe to 50 Oe in agreement with previous results.[25,27,28] The reason for the in-plane uniaxicity comes from the co-sputtering deposition method[29] and its magnetic easy axis (E.A.) is parallel to the short side of the magnetic frames [Fig. 1(a)]. In the patterned sample, the behavior indicated by the control films is confirmed, as can be observed from the remanence magnetic force microscopy image of a disc and its surrounding etched film [Fig. 1(d)]. The signal from the disc shows magnetic stripe domains and the etched film around it not, thus we have fabricated an exchange coupled 2D hard-soft system, where the discs present a PMA magnetic material behavior with weak magnetic stripe domains[17,22,30] and the rest of the layer exhibits an in-plane uniaxial magnetization behavior. The magnetic differences between the discs and the etched layer allow us to perform the following experiment to control the magnetization reversal in this last one: first, by the application of an in-plane saturating field ($H \geq 1500$ Oe) we can orient the weak magnetic stripe domains in the discs along the field direction,[23,25] and second, measure the hysteresis loops of the etched layer in the in-plane E.A. direction with a field amplitude smaller than 150 Oe which, according to the hysteresis loops of the control layers shown in Fig. 1(c), should be enough to reverse the etched layer keeping the discs magnetization orientation unchanged. The selected saturation senses are positive (→) and negative (←), both parallel to E.A., and also perpendicular (↑).

In Figure 2, the hysteresis loops of the sample with a lattice parameter $L = 7.5\,\mu m$ are presented with domain images taken simultaneously to the acquisition of the loops by Kerr Microscopy (KM).[22] Images and loops are measured

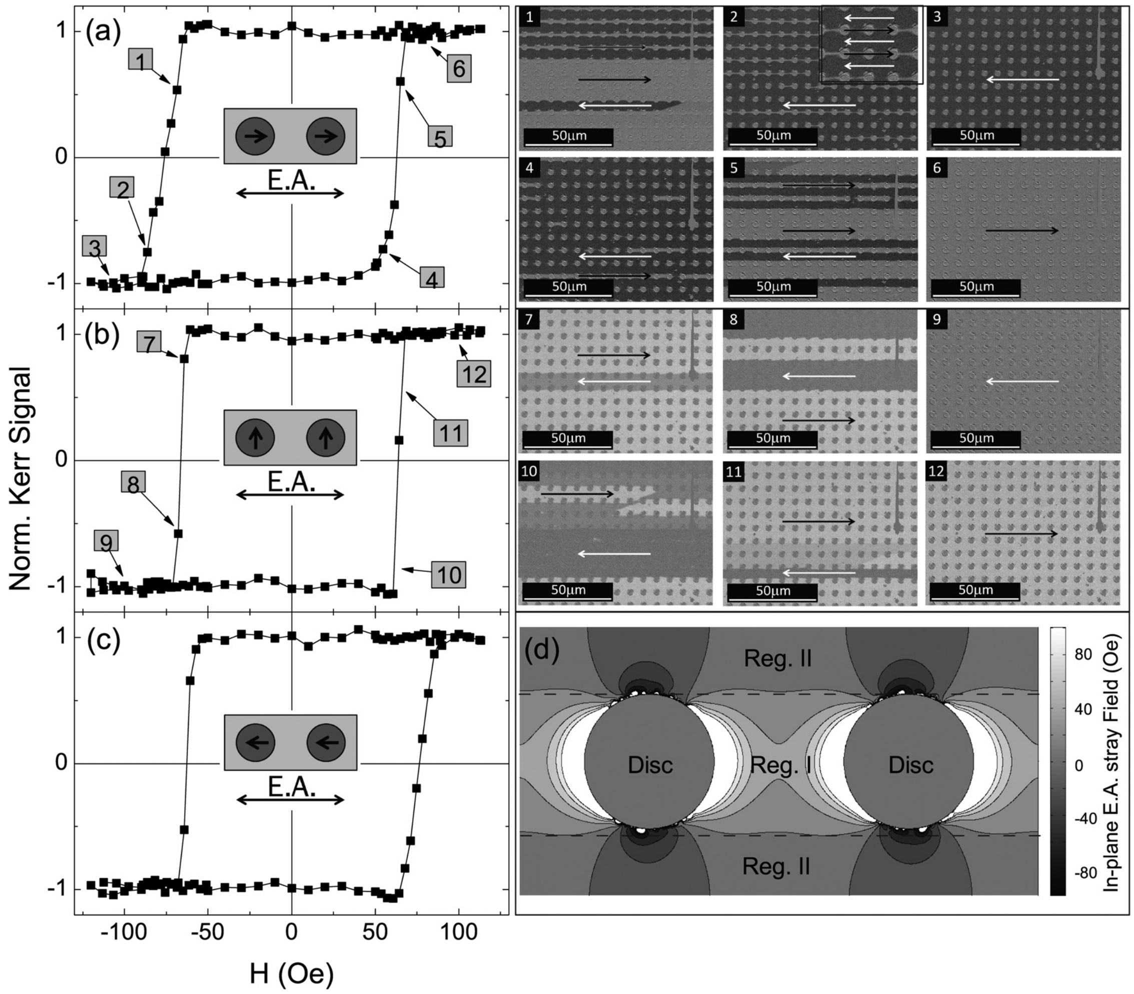

FIG. 2. Kerr microscopy hysteresis loops and domain images of the sample with lattice parameter $L = 7.5\,\mu$m after disc's in-plane magnetization orientation parallel positive [(a), images (1–6)], perpendicular [(b), images (7–12)], and parallel negative [(c), images not shown] to E.A. (schemes at inset of hysteresis loops). (d) Stray field map at remanence along the E.A. (H_{stray}) obtained by micromagnetic calculations for an array of discs with $L = 6\,\mu$m. Regions I and II correspond to inter-disc and linear areas in between the rows of discs, respectively.

following the previous method: after positive E.A. [Fig. 2(a) (1–6)], perpendicular to E.A. [Fig. 2(b) (7–12)] and negative E.A. [Fig. 2(c), images not shown] saturations. Dark and bright grey contrasts in KM images indicate in-plane magnetization domains pointing to the left (←, white arrows) and right (→, black arrows), respectively, and the magnetic field direction applied during the loop measurement is parallel to the etched layer E.A., which is parallel to the arrows in the images. The jump on the Kerr signal has been normalized between the positive and negative saturation senses of the etched layer. The NdCo discs keep their image color (same orientation of the in-plane M component) during the whole $M(H)$ loop of the etched layer, which should introduce a vertical shift in the $M(H)$ cycle, as reported in Ref. 16.

An asymmetry in the backward and forward branches of the hysteresis loops and an "exchange bias-like" field shift (this last one calculated as half the difference between the coercive fields of the loops) can be observed in the positive [Fig. 2(a)] and negative [Fig. 2(c)] E.A. orientations, respectively, while in the perpendicular one, no bias-field shift is observed and the loop keeps its symmetry [Fig. 2(b)]. Thus, the system exhibits a tunable "exchange bias-like" effect, which is a very interesting feature in exchange bias standard vertical multilayers.[11,31] Our results show a similar behavior than those reported in Refs. 12 and 16 but with external applied magnetic fields needed to tune the exchange bias effect at least one order of magnitude lower (10^3 Oe) than those used (10^4–10^5 Oe) in Refs. 12 and 16.

The observed tunable exchange bias-like effect can be linked to coupling effects between the discs and the etched layer. In general, the coupling in laterally patterned structures is caused by exchange at the interfaces and magnetostatic charges created by the lateral modulation of in-plane magnetization.[30] In the present case, KM images indicate significant differences in the magnetization reversal of inter-disc areas [labeled as I in Fig. 2(d)] and of the linear regions in between the rows of discs [labeled as II in Fig. 2(d)]. In the case of positive E.A. orientation, regions II reverse first, while regions I remain with the original magnetization orientation [Fig. 2(a) (1–2)]. A field of −100 Oe is needed to completely remove these inter-disc domains. The second magnetization reversal shows the opposite behavior: the first reversed domains appear at regions I [Fig. 2(a) (4)] and, then, expand into regions II [Fig. 2(a) (5)], and the final field to saturate the etched layer is reduced to 70 Oe. The same behavior is observed in the negative E.A. orientation of the discs in-plane magnetization, but in the opposite order. These different magnetic domains behaviors are responsible of the asymmetries observed in the branches of the $M(H)$ loops. In the case of perpendicular to E.A. orientation, no inter-disc domains are observed during the whole magnetization reversal process [Fig. 2(b) (7–12)]. Regions I and II are directly connected with the configuration of the stray field created by the array of discs. We have performed micromagnetic simulations by using Mumax 3.5 (Ref. 32) of the magnetic configuration of the array of discs ($L = 6\,\mu$m) after saturating them in-plane and along the positive E.A. direction. The simulation was done using an exchange stiffness of 10^{-6} erg/cm, a PMA energy density of 10^6 erg/cm^3 and a saturation magnetization of 10^3 emu/cm^3. Figure 2(d) shows a map of the calculated stray field (H_{stray}) along the E.A. created by the discs in regions I and II at remanence after saturating them at the positive direction. Region I corresponds to a positive stray field, whereas in regions II, H_{stray} changes between positive and negative values. The local stray field in the center of region I has positive values of 40 Oe at discs remanence and 17 (22) Oe at forward (backward) coercive field (H_c). Therefore, we have always a significant positive bias field in region I, indicating that magnetostatic interactions alone can introduce a shift in the hysteresis loop. However, in the presented system, the exchange interaction between the discs and the etched layer should also play a role in the observed exchange bias-like effect. In Table I, the experimental forward (H_c^+) and backward (H_c^-) coercive fields and bias field (H_b) as a function of sample lattice parameters (L) are presented for the three different disc's in-plane magnetization orientations: parallel [positive (→) and negative (←)] and perpendicular (↑) to E.A. The applied magnetic field amplitude during the measurement of the hysteresis loops is 150 Oe for the sample with $L = 6\,\mu$m and 120 Oe for the others.

The existence of a switchable bias field shift is observed in all the fabricated samples due to the same magnetic domain's behavior during the magnetization reversal processes. This shift can be understood in terms of exchange and magnetostatic interactions between the discs and the surrounding etched layer, mainly because of the in-plane magnetization discontinuities at the discs edges.[30] The discs act as nucleation points for the domains in the etched layer with the same orientation than the discs in-plane magnetization (→ or ←), and because of the stray field generated at the edges, a faster (stronger) growth (pinning) of reversed (original) inter-disc domains takes place. Due to its magnetostatic origin, we can tune the magnitude of the bias field by changing the lattice parameter of the system as illustrated in Table I, where the sample with $L = 9\,\mu$m shows a H_b of 4.5 Oe, which is smaller than the bias field of the $L = 7.5\,\mu$m sample (7.0 Oe). However, not only the lattice parameter controls the strength of H_b, but also the maximum amplitude of the applied magnetic field during the measurement of the hysteresis loop of the etched layer seems to play an important role. In the case of the sample with $L = 6\,\mu$m, a field amplitude of 150 Oe has been used to completely saturate the etched layer (because of the higher strength of the bias field). We think that the effect of this higher applied field amplitude induces a different minor loop in the discs so that the recorded in-plane magnetization component is reduced, originating a smaller stray field that contributes to the bias field decrease. This phenomenon was also observed in Refs. 13 and 16 for a system consisting of two perpendicularly coupled ferromagnets.

TABLE I. Forward (H_c^+) and backward (H_c^-) coercive and bias (H_b) fields obtained from the hysteresis loops for different disc's in-plane magnetization orientations, namely, parallel [positive (→) and negative (←)] and perpendicular (↑) to E.A. for different lattice parameters (L). Applied magnetic field amplitudes during the measurement of the loops are 150 Oe for $L = 6\,\mu$m and 120 Oe for $L = 7.5\,\mu$m and $L = 9\,\mu$m.

H (Oe) \ L (μm)	6.0	7.5	9.0
H_c^+ (→)	70 ± 1	62 ± 1	61 ± 1
H_c^- (→)	−81 ± 1	−76 ± 1	−70 ± 1
H_b (→)	−5.5 ± 1	−7.0 ± 1	−4.5 ± 1
H_c^+ (←)	82 ± 1	76 ± 1	70 ± 1
H_c^- (←)	−70 ± 1	−62 ± 1	−61 ± 1
H_b (←)	6.0 ± 1	7.0 ± 1	4.5 ± 1
H_c^+ (↑)	67 ± 1	64 ± 1	62 ± 1
H_c^- (↑)	−69 ± 1	−66 ± 1	−63 ± 1
H_b (↑)	−1.0 ± 1	−1.0 ± 1	−0.5 ± 1

In summary, we have fabricated patterned 2D $NdCo_5$-based magnetic lateral hard-soft composites with PMA, where the thickness of the $NdCo_5$ layer is laterally modulated so that soft (hard) regions are below (above) the critical thickness for nucleation of weak stripe domains in the system. This spatial modulation of the magnetic behavior leads to an exchange coupled system, which exhibits a tunable "exchange bias-like" shift in the $M(H)$ hysteresis loops of the thin $NdCo_5$ etched layer, switchable (on/off) by the orientation of the weak stripe domains of the thick $NdCo_5$ discs that are controlled by the last saturating magnetic field.

Work supported by Spanish MINECO under Grant Nos. FIS2008-06249 and FIS2013-45469. A. Hierro-Rodriguez and J. M. Teixeira acknowledge support from FCT of Portugal (Grant Nos. SFRH/BPD/90471/2012 and SFRH/BPD/72329/2010, respectively).

[1]D. A. Allwood, G. Xiong, M. D. Cooke, C. C. Faulkner, D. Atkinson, N. Vernier, and R. P. Cowburn, Science **296**, 2003 (2002).
[2]D. A. Allwood, G. Xiong, and R. P. Cowburn, Appl. Phys. Lett. **89**, 102504 (2006).
[3]G. Rodríguez-Rodríguez, A. Pérez-Junquera, M. Vélez, J. V. Anguita, J. I. Martín, H. Rubio, and J. M. Alameda, J. Phys. D: Appl. Phys. **40**, 3051 (2007).
[4]M. Hayashi, L. Thomas, R. Moriya, C. Rettner, and S. S. P. Parkin, Science **320**, 209 (2008).
[5]A. Pérez-Junquera, V. I. Marconi, A. B. Kolton, L. M. Álvarez-Prado, Y. Souche, A. Alija, M. Vélez, J. V. Anguita, J. M. Alameda, J. I. Martín *et al.*, Phys. Rev. Lett. **100**, 037203 (2008).
[6]K.-J. Kim, J.-C. Lee, S.-J. Yun, G.-H. Gim, K.-S. Lee, S.-B. Choe, and K.-H. Shin, Appl. Phys. Exp. **3**, 083001 (2010).
[7]J. Münchenberger, G. Reiss, and A. Thomas, J. Appl. Phys. **111**, 07D303 (2012).
[8]S. P. Li, W. S. Lew, J. A. C. Bland, L. Lopez-Diaz, C. A. F. Vaz, M. Natali, and Y. Chen, Phys. Rev. Lett. **88**, 087202 (2002).
[9]J. McCord, L. Schultz, and J. Fassbender, Adv. Mater. **20**, 2090 (2008).
[10]K. Theis-Bröhl, M. Wolff, A. Westphalen, H. Zabel, J. McCord, V. Höink, J. Schmalhorst, G. Reiss, T. Weis, D. Engel *et al.*, Phys. Rev. B **73**, 174408 (2006).
[11]J. Nogués and I. K. Schuller, J. Magn. Magn. Mater. **192**, 203 (1999).
[12]J. Nogués, J. Sort, S. Suriñach, J. S. Muñoz, M. D. Baró, J. F. Bobo, U. Lüders, E. Haanappel, M. R. Fitzsimmons, A. Hoffmann *et al.*, Appl. Phys. Lett. **82**, 3044 (2003).

[13]A. Bollero, B. Dieny, J. Sort, K. S. Buchanan, S. Landis, and J. Nogués, Appl. Phys. Lett. **92**, 022508 (2008).
[14]A. Bollero, V. Baltz, L. D. Buda-Prejbeanu, B. Rodmacq, and B. Dieny, Phys. Rev. B **84**, 094423 (2011).
[15]D. Navas, J. Torrejon, F. Béron, C. Redondo, F. Batallan, B. P. Toperverg, A. Devishvili, B. Sierra, F. Castaño, K. R. Pirota *et al.*, New J. Phys. **14**, 113001 (2012).
[16]J. Sort, A. Popa, B. Rodmacq, and B. Dieny, Phys. Rev. B **70**, 174431 (2004).
[17]A. Hierro-Rodriguez, R. Cid, M. Vélez, G. Rodriguez-Rodriguez, J. I. Martín, L. M. Álvarez-Prado, and J. M. Alameda, Phys. Rev. Lett. **109**, 117202 (2012).
[18]A. F. Rodríguez, L. J. Heyderman, F. Nolting, A. Hoffmann, J. E. Pearson, L. M. Doeswijk, M. A. F. van den Boogaart, and J. Brugger, Appl. Phys. Lett. **89**, 142508 (2006).
[19]S. Sievers, S. Schnittger, J. Norpoth, X. Hu, U. Siegner, H. W. Schumacher, and C. Jooss, J. Appl. Phys. **110**, 043927 (2011).
[20]P. J. Metaxas, P.-J. Zermatten, R. L. Novak, S. Rohart, J.-P. Jamet, R. Weil, J. Ferré, A. Mougin, R. L. Stamps, G. Gaudin *et al.*, J. Appl. Phys. **113**, 073906 (2013).
[21]See supplementary material at http://dx.doi.org/10.1063/1.4895771 for more details about the magnetic properties of weak PMA materials.
[22]A. Hubert and R. Shäfer, *Magnetic Domains* (Springer, Berlin, 1998).
[23]H. Fujiwara, Y. Sugita, and N. Saito, Appl. Phys. Lett. **4**, 199 (1964).
[24]L. M. Alvarez-Prado, G. T. Pérez, R. Morales, F. H. Salas, and J. M. Alameda, Phys. Rev. B **56**, 3306 (1997).
[25]A. Hierro-Rodriguez, G. Rodríguez-Rodríguez, J. M. Teixeira, G. N. Kakazei, J. B. Sousa, M. Vélez, J. I. Martín, L. M. Alvarez-Prado, and J. M. Alameda, J. Phys. D: Appl. Phys. **46**, 345001 (2013).
[26]C. Dehesa-Martínez, L. Blanco-Gutierrez, M. Vélez, J. Díaz, L. M. Alvarez-Prado, and J. M. Alameda, Phys. Rev. B **64**, 024417 (2001).
[27]R. Cid, G. Rodríguez-Rodríguez, L. M. Álvarez-Prado, J. Díaz, and J. M. Alameda, J. Magn. Magn. Mater. **316**, e446–e449 (2007)
[28]E. S. Leva, R. C. Valente, F. M. Tabares, M. V. Mansilla, S. Roshdestwensky, and A. Butera, Phys. Rev. B **82**, 144410 (2010).
[29]J. M. Alameda, F. Carmona, F. H. Salas, L. M. Alvarez-Prado, R. Morales, and G. T. Pérez, J. Magn. Magn. Mater. **154**, 249 (1996).
[30]A. Hierro-Rodriguez, M. Vélez, R. Morales, N. Soriano, G. Rodríguez-Rodríguez, L. M. Álvarez-Prado, J. I. Martín, and J. M. Alameda, Phys. Rev. B **88**, 174411 (2013).
[31]C. Binek, S. Polisetty, X. He, and A. Berger, Phys. Rev. Lett. **96**, 067201 (2006).
[32]A. Vansteenkiste, B. Van de Wiele, L. Dupré, B. Van Waeyenberge, and D. De Zutter, Int. J. Numer. Modell. Electron. Networks Devices Fields **26**, 366 (2013).